Polymer Chemistry

Accepted Manuscript

ROYAL SOCIETY OF CHEMISTRY

www.rsc.org/polymers

Cite this: DOI: 10.1039/c0xx00000x

www.rsc.org/xxxxxx

ARTICLE TYPE

Effect of Cyano (CN)–group on the Planarity, Film Morphology and Photovoltaic Performance of Benzodithiophene–Based Polymers†

Jialing Lu,[a] Jianyu Yuan,[a] Wenping Guo,[b] Xiaodong Huang,[a] Zeke Liu,[a] Haibing Zhao,[b] Hai-Qiao Wang*[a] and Wanli Ma*[a]

Received (in XXX, XXX) Xth XXXXXXXXX 20XX, Accepted Xth XXXXXXXXX 20XX
DOI: 10.1039/b000000x

A class of polymers (**POT–DH**, **POT–HCN** and **POT–DCN**) were synthesized and they contain the same donor (BDT) and acceptor unit but incorporated with different number of cyano (CN)–groups, i.e. 0, 1 and 2. We investigated for the first time the effects of different CN−group numbers on the optoelectronic, molecule packing, film morphology and photovoltaic properties of three conjugated polymers. With increased CN−group number, broader absorption, smaller optical bandgap and lower HOMO level can be obtained. The planarity of polymers also decreases with increased CN−group, leading to different inter−molecular packing and morphology. The incorporation of two CN−groups results in poor morphology, inefficient charge transfer and very low device performance. Due to the optimized **POT–HCN** polymer possessing the most balanced properties, the best PCE of 4.21% was demonstrated by **POT−HCN** with one CN−group. Thus we believe that, by controlling the number of introduced CN−groups, we can generally fine−tune the planarity and LUMO/HOMO levels of this class of polymers to achieve desired optoelectronic properties and morphology for high photovoltaic performance. This also provides a feasible way for optimizing other photovoltaic semiconducting polymers by adjusting the number of electron–withdrawing unit.

Introduction

As a potential and promising renewable energy source, bulk heterojunction (BHJ) polymer solar cell (PSC) has attracted significant attention recently.[1] However, up to now the device power conversion efficiency (PCE) still remains one of the key factors hindering its practical application. It is well–known that the PCE is proportional to the open circuit voltage (V_{oc}), short circuit current density (J_{sc}) and fill factor (*FF*) of PSCs. To obtain high V_{oc}, J_{sc}, and *FF*, many efforts have been devoted to modify the chemical structure of conjugated polymers to tune their optoelectronic properties, and consequently improve the performance of PSCs. Generally, the structural modifications have been focused on adjusting the solubilizing alkyl group,[2] conjugated substituent group[3] and polymer backbone.[4] However, the incorporation of electron–withdrawing groups in D–A type polymer, such as cyano (CN)–group,[5] fluorine moiety,[3c,6] carbonyl–group and carboxyl–group,[7] can also significantly affect the physical and chemical properties of modified polymer, such as solubility, crystallinity, absorbance, electrochemical and interchain–packing properties. Specifically, as a strong electron–withdrawing unit, CN–group has been widely adopted in small molecules.[8] CN–group can significantly lower the LUMO (the lowest unoccupied molecular orbital) level while only lowering the HOMO (the highest occupied molecular orbital) level slightly,[5a] resulting in changes in small molecule's physical, electrochemical properties and photovoltaic performance.[8a-d] For example, Li and coworkers have reported that the introduction of CN–group into a small molecule's backbone lowered both the LUMO and HOMO energy levels, leading to significantly increased PCE from 1.99% to 3.85%.[8d] However, compared to the successful application in small molecules,[8a-e] the use of CN–group in polymers for OPV application has only limited success.[5e-g] Therefore, more investigations may be required to better understand the effect of CN–group on the properties and photovoltaic performance of conjugated polymers.

In our previous work,[9] we designed and synthesized four new homologous polymers, composed of benzo[1,2b:4,5b□]dithiophene (BDT) donor and fumaronitrile (BCNV) acceptor comonomers with different π–bridges. Two CN–groups were introduced to all the four polymers to achieve desired physical, electrochemical properties and high photovoltaic performance. Although broadened absorption and high V_{oc} were achieved, the devices only demonstrated extremely low PCEs. We concluded that it is mainly due to the polymer relatively low LUMO levels and poor backbone planarity, induced by the CN–groups. Thus we proposed to optimize the number of CN–groups in the polymer structure to achieve the proper LUMO energy levels to provide sufficient downhill driving force for the exciton dissociation. In addition, the polymer planarity could also be changed by the number of introduced CN–groups, consequently affecting the inter–molecular packing and the morphology of the formed film.[5b-d]

Based on the above consideration, three polymers (**POT–DH**, **POT–HCN** and **POT–DCN**) were synthesized, which contain the same donor (BDT) and acceptor unit but incorporated with different number of CN–groups, i.e. 0, 1 and 2. The effects of the different CN–group numbers on polymers' optoelectronic, molecule packing, film morphology and photovoltaic performance were systematically investigated. By adjusting the CN–group, we have achieved semiconducting polymers with improved absorption range, HOMO/LUMO levels and backbone planarity compared to our previously reported polymers.[9]

Experimental

Materials and instruments

Toluene and THF were dried over sodium/benzophenone ketyl and distilled before using. DMF was distilled over CaH_2. Chloroform, methanol and dichloromethane were used as received. PEDOT:PSS (Clevios P VP .Al 4083) used for the fabrication of PSCs was purchased from Heraeus. Thiophene-2-carbaldehyde, 2-(thiophen-2-yl)acetonitrile and all other chemicals were purchased from Sigma–Aldrich and used as received without further purification, unless other noted. 2,6-Bis(trimethyltin)-4,8-di(2-octyldodecyloxy)-benzo[1,2-b;3,4-b]-dithiophene (**D**) was prepared according to the literature.[10]

^{1}H NMR and ^{13}C NMR data were respectively performed on a Varian Unity Inova 400 MHz and a Varian NMR system 300 MHz spectrometer with tetramethylsilane (TMS; δ=0 ppm) as the internal standard. GC–MS spectra were obtained by using a ThermoFisher Scientific GC/MS Trace–ISQ mass spectrometer. Thermo gravimetric analysis (TGA) was carried out by using a Perkin Elmer TGA4000 at a heating rate of 10 °C/min in nitrogen atmosphere. Molecular weight and molecular weight distribution (PDI) were determined against a polystyrene standard by gel permeation chromatography (GPC) on a PL–GPC 50 apparatus, and THF was used as the eluent at a flow rate of 1.0 ml/min at 40 °C. UV–vis–NIR spectra were recorded on a Perkin Elmer model Lambda 750 instrument. Cyclic voltammetric (CV) measurements were carried out using a Zahner IM6 electrochemical workstation. Tapping–mode AFM images were obtained with a Veeco Multimode V instrument. Transmission electron microscopy (TEM) images and high-angle annular dark–field scanning transmission–electron microscopy (HAADF–STEM) images were obtained by using a Tecnai G2 F20 S–Twin transmission electron microscope.

Fabrication and characterization of polymer solar cells and hole–only devices

PSCs were fabricated with a general structure of ITO/PEDOT–PSS (40 nm)/polymer:PCBM/LiF (0.6 nm)/Al (100 nm). Patterned ITO substrates were cleaned by ultrasonic treatment sequentially in detergent–water, acetone, deionized water and isopropyl alcohol, and finally treated by UV–ozone for 20 min. The PEDOT:PSS (~40 nm) was spin–coated on ITO substrates and dried at 150 °C for 20 min. Then, blends of polymers and PCBM with different ratios were dissolved in chloroform or CB with or without DIO (2% v/v), the solutions were filtered through a 0.45 μm poly(tetrafluoroethylene) (PTFE) filter. After deposition of the active layers with different spin–coating speeds for 40 s, 0.6 nm of LiF (0.1 Å/s) and 100 nm Al (2 Å/s) layers were thermally evaporated on the active layer at a pressure of 1.0×10^{-6} m bar through a shadow mask (active area 7.25 mm^2). The current density–voltage characteristics of the polymer solar cells were measured by using a Keithley 2400 (I–V) digital source meter under a simulated AM 1.5 G solar irradiation at 100 mW cm^{-2} (Newport, Class AAA solar simulator, 94023A–U).

Hole–only devices were fabricated to measure the hole mobility of polymers by the space charge limited current (SCLC) method. The device structure was ITO/ZnO/polymer:$PC_{61}BM$/MoO_3/Al. The mobility is determined by fitting the dark current to the model of a single carrier SCLC, which is described by the equation:[11]

$$J = \frac{9}{8}\varepsilon_0\varepsilon_r\mu_h\frac{V^2}{d^3},$$

where J is the current, μ_h is the zero–field mobility, ε_0 is the permittivity of free space, ε_r is the relative permittivity of the material, d is the thickness of the active layer, and V is the effective voltage. The effective voltage can be obtained by subtracting the built–in voltage (V_{bi}) and the voltage drop (V_s) from the substrate's series resistance from the applied voltage (V_{appl}), $V=V_{appl}-V_{bi}-V_s$.

Synthesis of monomers and polymers

1,2-di(thiophen-2-yl)ethane (1). Zinc powder (17.39 g, 267.50 mmol) was dissolved in anhydrous THF (250 ml) in a dry two-neck flask, and $TiCl_4$ (25.37 g, 133.74 mmol) was added dropwise to the solution at 0 °C. Then, a solution of thiophene-2-carbaldehyde (5 g, 44.58 mmol) in anhydrous THF (50 ml) was added into the reaction solution at 0 °C. The reaction mixture was vigorously stirred at 70 °C for 5 h. Then the reaction mixture was poured into a separating funnel with aqueous $NaHCO_3$ solution, and then the aqueous layer was extracted with methylene chloride while the combined organic layer was dried over an hydrous Na_2SO_4 and concentrated under reduced pressure to give the crude product. Finally, the pure product was recrystallized from ethanol as a light yellow powder (3.10 g) with a yield of 72.3%. ^{1}H NMR (400 MHz, $CDCl_3$, δ, ppm): 7.19 (d, 2H), 7.06 (d, 2H), 7.04 (d, 2H), 7.00 (d, 2H). ^{13}C NMR (400 MHz, $CDCl_3$, δ, ppm): 142.5, 127.8, 126.1, 124.4, 121.6. GC–MS ($C_{10}H_8S_2$): calcd, 192.30; found, 192.24.

5-bromothiophene-2-carbaldehyde (2). In a dry two–neck 100 ml round bottom flask, thiophene-2-carbaldehyde (5.00 g, 44.58 mmol) was dissolved in anhydrous N, N-dimethylformamide (DMF) (30 ml) under argon. After N-bromosuccinimide (NBS) (7.94 g, 44.58 mmol) was added slowly over 15 min, the reaction mixture was stirred at room temperature in dark overnight. Then the reaction mixture was poured into water (300 ml) and extracted with chloroform (3 × 50 ml). The extracts were combined and washed with water and then dried over anhydrous Na_2SO_4. After filtration, the solvent was removed under vacuum. The residue was further purified by column chromatography on silica using petroleum ether (60–90 °C) and ethyl acetate (v/v=15:1) as eluent to afford compound **2** (7.10 g, 83.3%) as orange oil. ^{1}H NMR (400 MHz, $CDCl_3$, δ, ppm): 9.74 (s, 1H), 7.50 (d, 1H), 7.16 (d, 1H). ^{13}C NMR (400 MHz, $CDCl_3$, δ, ppm): 181.7, 145.1, 136.5, 131.4, 124.9. GC–MS (C_5H_3BrOS): calcd, 191.05; found, 190.98.

2-(5-bromothiophen-2-yl)acetonitrile (3). In a dry two–neck

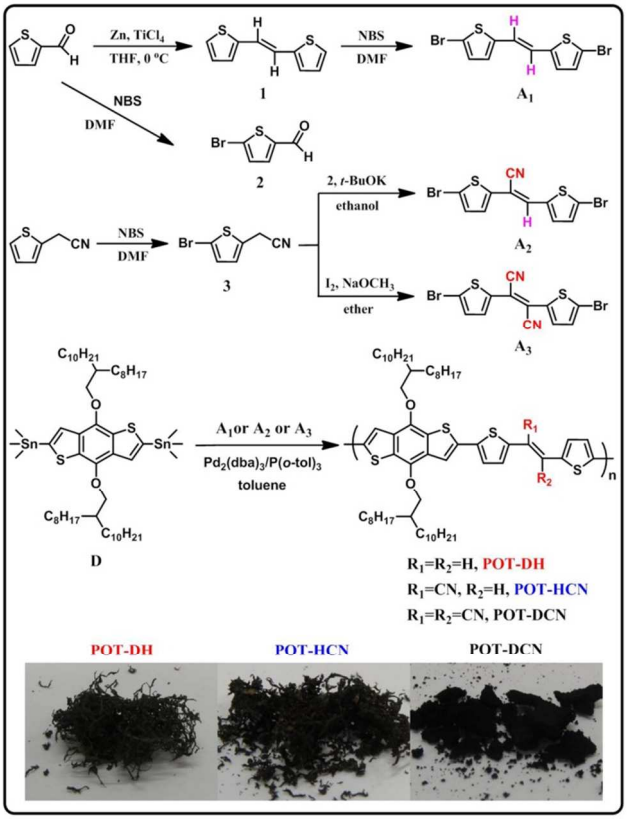

Scheme 1 Structure and synthesis route of monomers and polymers; inset: different facade of three polymers.

100 ml round bottom flask, 2-(thiophen-2-yl)acetonitrile (4.00 g, 32.47 mmol) was dissolved in anhydrous DMF (30 ml) under argon. NBS (6.07 g, 34.10 mmol) was added slowly over 15 min, the reaction mixture was stirred at room temperature in dark overnight. Then the reaction mixture was poured into water (300 ml) and extracted with chloroform (3 × 50 ml). The extracts were combined and washed with water and then dried over anhydrous Na_2SO_4. After filtration, the solvent was removed under vacuum. The residue was further purified by column chromatography on silica using petroleum ether (60–90 °C) and ethyl acetate (v/v=15:1) as eluent to afford compound **3** (5.36 g, 81.3%) as light yellow oil. ^{1}H NMR (300 MHz, $CDCl_3$, δ, ppm): 6.94 (d, 1H), 6.83 (d, 1H), 3.84 (s, 2H). ^{13}C NMR (300 MHz, $CDCl_3$, δ, ppm): 132.4, 130.1, 127.7, 118.4, 112.3, 18.8.

1,2-bis(5-bromothiophen-2-yl)ethane (A_1). In a dry two-neck 100 ml round bottom flask, compound **1** (3.10 g, 16.12 mmol) was dissolved in anhydrous DMF (30 ml) under argon. After NBS (5.74 g, 32.24 mmol) was added slowly over 15 min, the reaction mixture was stirred at room temperature in dark overnight. Then the reaction mixture was poured into water (300 ml) and extracted with chloroform (3 × 50 ml). The extracts were combined and washed with water and then dried over anhydrous Na_2SO_4. After filtration, the solvent was removed under vacuum. The residue was further purified by column chromatography on silica using petroleum ether (60–90 °C) as eluent to afford $\mathbf{A_1}$ (4.4 g, 78.0%) as yellow solid. ^{1}H NMR (400 MHz, $CDCl_3$, δ, ppm): 6.93 (d, 2H), 6.79 (d, 2H), 6.76 (d, 2H). ^{13}C NMR (400 MHz, $CDCl_3$, δ, ppm): 143.6, 130.6, 126.6, 121.1, 111.5. GC–MS ($C_{10}H_6Br_2S_2$): calcd, 350.09; found, 349.92.

2,3-bis(5-bromothiophen-2-yl)acrylonitrile (A_2). Compound **2** (2.00 g, 10.47 mmol) and compound **3** (2.12 g, 10.47 mmol) were dissolved in anhydrous ethanol under nitrogen and then *t*-BuOK (200 mg) was added. The reaction mixture was vigorously stirred at room temperature overnight. Then the reaction mixture was poured into water (300 ml) and extracted with chloroform (3 × 50 ml). The extracts were combined and washed with water and then dried over anhydrous Na_2SO_4. After filtration, the solvent was removed under vacuum. The crud product was further purified by recrystallizing from methylene dichloride to afford pure $\mathbf{A_2}$ (3.15 g) as yellow solid with a yield of 80.2%. ^{1}H NMR (400 MHz, $CDCl_3$, δ, ppm): 7.39 (s, 1H), 7.27 (d, 1H), 7.21 (d, 1H), 7.09 (d, 1H), 7.03 (d, 1H). ^{13}C NMR (400 MHz, $CDCl_3$, δ, ppm): 139.8, 139.0, 137.9, 135.1, 133.2, 131.4, 131.0, 130.2, 127.5, 118.9, 116.5. GC–MS ($C_{11}H_5Br_2NS_2$): calcd, 375.10; found, 374.94.

2,3-bis(5-bromothiophen-2-yl)fumaronitrile (A_3). Compound **3** (4.00 g, 19.80 mmol) and iodine (5.03 g, 19.82 mmol) were dissolved in 80 ml anhydrous diethyl ether and the solution was cooled down to –78 °C by a liquid anhydrous alcohol bath under argon. Then a cooled solution (–78 °C) of sodium methoxide (2.55 g, 45.54 mmol) in methanol (40 ml) was added dropwise with stirring over 30 min. After being stirred for 2 h at –78 °C, the mixture was maintained at 0 °C for 5 hours with stirring. Then the mixture was acidified by addition of dilute HCl (aq) (3%, v/v, 50 ml) and the resultant precipitate was filtered on a sinter. The crude product was washed on the sinter with water (3×100 ml) and ethanol (3×100 ml). Further purification was carried out by recrystallization using ethanol to obtain the pure compound $\mathbf{A_3}$ (1.28 g, 16.2%) as black solid. ^{1}H NMR (400 MHz, $CDCl_3$, δ, ppm): 7.58 (d, 2H), 7.16 (d, 2H). ^{13}C NMR (400 MHz, $CDCl_3$, δ, ppm): 134.38, 133.70, 131.09, 130.98, 121.37, 120.19. GC–MS ($C_{12}H_4Br_2N_2S_2$): calcd, 400.11; found, 399.90.

Polymerization for POT–DH. In a 50 ml reaction tube, monomer **D** (0.250 g, 0.225 mmol), monomer $\mathbf{A_1}$ (0.079 g, 0.225 mmol), tri(o-tolyl)phosphine (0.020 g, 0.080 mmol) and $Pd_2(dba)_3$ (0.010 g, 0.010 mmol) were added. The mixture was subjected to three cycles of evacuation and substituted by argon. Then anhydrous toluene (6 ml) was injected in the reaction mixture through syringe. After being stirred for 24 h at 110 ºC, the reaction mixture was cooled down to room temperature and then precipitated in methanol (130 ml). The precipitate was filtered and repeatedly washed with methanol (24 h), hexane (24 h) and chloroform (12 h) in a Soxhlet apparatus. The chloroform fraction was concentrated and precipitated in methanol. The precipitate was filtered and dried in vacuum at 90 °C for 24 h. **POT–DH** (0.196 g) was obtained as dark red solid with a yield of 89.5%. GPC: M_n=24.09 kg/mol, M_w=60.61 kg/mol; PDI=2.52. ^{1}H NMR (300 MHz, $CDCl_3$, δ, ppm): 7.80–6.98 (br, 6H Ar H), 6.75 (br, 2H), 4.19 (br, 4H), 1.92–1.28 (br, 66H), 0.88 (br, 12H). Anal. Clacd for $C_{60}H_{90}O_2S_4$ (%): C, 74.10; H, 9.26; N, 0.00. Found: C, 74.32; H, 9.33; N, 0.00.

Polymerization for POT–HCN. POT–HCN was prepared from monomer **D** (0.250 g, 0.225 mmol) and monomer $\mathbf{A_2}$ (0.084 g, 0.225 mmol) by using the same method as for **POT–HCN** as dark blue solid with a yield of 87.3% (0.196 g). GPC: M_n=27.72 kg/mol, M_w=103.22 kg/mol; PDI=3.72. ^{1}H NMR (300 MHz, $CDCl_3$, δ, ppm): 7.80–6.76 (br, 6H Ar H, 1H), 4.17 (br, 4H),

Table 1 Molecular weights and thermal properties of the polymers.

Polymer	M_n (Kg/mol)[a]	M_w (Kg/mol)[a]	PDI[a]	T_d (°C)[b]
POT-DH	24.09	60.61	2.52	331
POT-HCN	27.72	103.22	3.72	341
POT-DCN	13.61	52.34	3.84	340

[a] Determined by GPC using polystyrene standards and THF as eluent. [b] 5% weight loss temperatures measured by TGA under nitrogen.

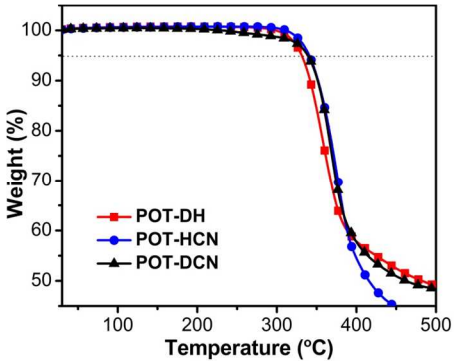

Fig. 1 TGA curves of the polymers with a heating rate of 10 °C/min under inert atmosphere.

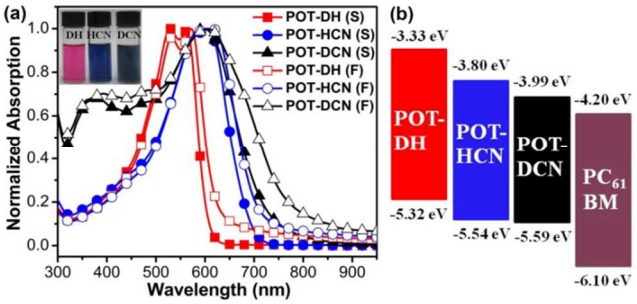

Fig. 2 (a) Normalized UV–vis. absorption spectra of polymers in dilute $CHCl_3$ solution (S) at room temperature and thin films (F) on quartz cast from $CHCl_3$ solutions of pure polymers. The inset shows the different colour of polymers in dilute $CHCl_3$ solutions. (b) Energy level diagrams of polymers and $PC_{61}CM$.

1.94–1.28 (br, 66H), 0.88 (br, 12H). Anal. Clacd for $C_{61}H_{89}NO_2S_4$ (%): C, 73.45; H, 8.93; N, 1.40. Found: C, 73.66; H, 9.05; N, 1.45.

Polymerization for POT–DCN. POT–DCN was prepared from monomer **D** (0.250 g, 0.225 mmol) and monomer $\mathbf{A_3}$ (0.090 g, 0.225 mmol) by using the same method as for **POT–DCN** as black solid with a yield of 81.9% (0.189 g). GPC: M_n=13.61 kg/mol, M_w=52.33 kg/mol; PDI=3.84. ^{1}H NMR (300 MHz, $CDCl_3$, δ, ppm): 7.89–6.94 (br, 6H Ar H), 4.24 (br, 4H), 1.88–1.28 (br, 66H), 1.28–0.81 (br, 12H). Anal. Clacd for $C_{62}H_{88}N_2O_2S_4$ (%): C, 72.82; H, 8.61; N, 2.74. Found: C, 72.93; H, 8.67; N, 2.77.

Results and discussion

Synthesis and thermal stability

The structure and synthetic route of the synthesized polymers are illustrated in Scheme 1. The detailed procedure is described in the experimental section. **POT–DH**, **POT–HCN** and **POT–DCN** were synthesized via Stille cross–coupling reaction. All polymers were obtained with high yields. The molecular weight was determined by gel permeation chromatography (GPC) analysis. The molecular weight and polydispersity index (PDI) of the polymers were listed in Table 1. **POT–DH** has a number–average molecular weight (M_n) of 24.09 kDa, with a PDI of 2.52. **POT–HCN** has a M_n of 27.72 kDa with a PDI of 3.72 and **POT–DCN** has a M_n of 13.61 kDa with a PDI of 3.84. They all exhibited good solubility in common solvents at room temperature, like chloroform (CF), chlorobenzene (CB) and *o*–dichlorobenzene (ODCB).

As shown in Fig. 1, all polymers exhibited good thermal stability under nitrogen atmosphere with the 5% weight–loss temperature (T_d) at 331, 341 and 340 °C, for **POT–DH**, **POT–HCN** and **POT–DCN**, respectively, which is important for their applications in PSCs. Obviously, the introduction of CN–groups improved polymer's thermal stability.

Optical and electrochemical properties

The UV–vis absorption of the polymers were investigated for both the dilute $CHCl_3$ solutions and the thin films spin–coated on quartz substrates (Fig. 2a) with corresponding data summarized in Table 2. As seen in Fig. 2a, the dilute solution of **POT–DH** in $CHCl_3$ shows narrow absorption ranging from 300 to 600 nm, while the **POT–HCN** and **POT–DCN** solutions show broader absorption band ranging from 300 to 750 nm. **POT–DH** has two peaks at 530 and 563 nm respectively, and **POT–HCN** just has a single shoulder at 605 nm, while **POT–DCN** has two shoulders at 380 and 596 nm respectively. Obviously, with the increase of CN–group number in polymer, the absorption range extends gradually toward the long wavelength region. Similar results were observed for the film absorptions. The film absorption edges of **POT–DH**, **POT–HCN** and **POT–DCN** are 623 nm, 713 nm, and 776 nm, indicating an optical bandgap of 1.99 eV, 1.74 eV and 1.60 eV, respectively. Therefore, the optical bandgaps of polymers were decreased with more CN–groups.

Cyclic voltammetry (CV) was used to measure the electrochemical properties of polymers (Fig. S1, see the ESI†). In the measurement, ferrocene was used as the internal standard ($E_{1/2(ferrocene)}$ = 0.71 V *vs* Ag/AgCl). The HOMO/LUMO levels of polymers were calculated according to the equation[12]: $E_{HOMO/LUMO} = [-(E_{onset}-0.71)-4.8]$ eV. As shown in Fig. 2b, with more CN–group numbers, the polymers show gradually decreased HOMO levels of –5.32, –5.54 and –5.59 eV for polymer **POT–DH**, **POT–HCN** and **POT–DCN** respectively, which is consistent with the result of the theoretical calculation (–4.78, –5.03 and –5.30 eV for the same three polymers respectively, see Fig. S2 in the ESI†). In short, for the three polymers, relatively deep HOMO levels are realized due to the effect of BDT unit and the CN–groups, indicating a high V_{oc} for the PSCs.

X–ray analysis and theoretical calculation

The effect of CN–group number on the polymer inter–molecular packing was investigated via grazing–incidence X–ray diffraction (GIXD) measurement. The GIXD patterns of **POT–DH**, **POT–HCN** and **POT–DCN** are shown in Fig. 3a. The (010) peak corresponding to π–π stacking is more prominent in the out–of–plane direction, which suggests that most of the polymer π–faces are oriented parallel to the substrates (inset, Fig. 3a). This face–

Table 2 Optical and electrochemical parameters of polymers.

Polymer	λ_{max} (nm)		λ_{onset} (nm)		E_g^{opt}	E_{ox}	E_{red}	HOMO	LUMO$^{(elec)}$	LUMO$^{(opt)}$
	Solution	Film	Solution	Film	(eV) [a]	(V) [b]	(V) [b]	(eV) [c]	(eV) [c]	(eV) [d]
POT-DH	530, 563	533, 572	606	623	1.99	1.23	-0.62	-5.32	-3.47	-3.33
POT-HCN	605	611	687	713	1.74	1.45	-0.65	-5.54	-3.44	-3.80
POT-DCN	380, 596	392, 605	730	776	1.60	1.50	-0.35	-5.59	-3.74	-3.99

[a] E_g^{opt} is determined by the absorption onset of polymers as thin films, $E_g^{opt}=1240/\lambda_{onset}$. [b] E_{ox} is the onset of the oxidation potential and E_{red} is onset of the reduction potential. [c] The HOMO/LUMO$^{(elec)}$ energy level is calculated by equation HOMO/LUMO$^{(elec)}$=[−(E_{ox}/E_{red}–0.71)–4.80] (eV). [d] the LUMO$^{(opt)}$ energy level is calculated by equation LUMO = E_g^{opt}+ HOMO.

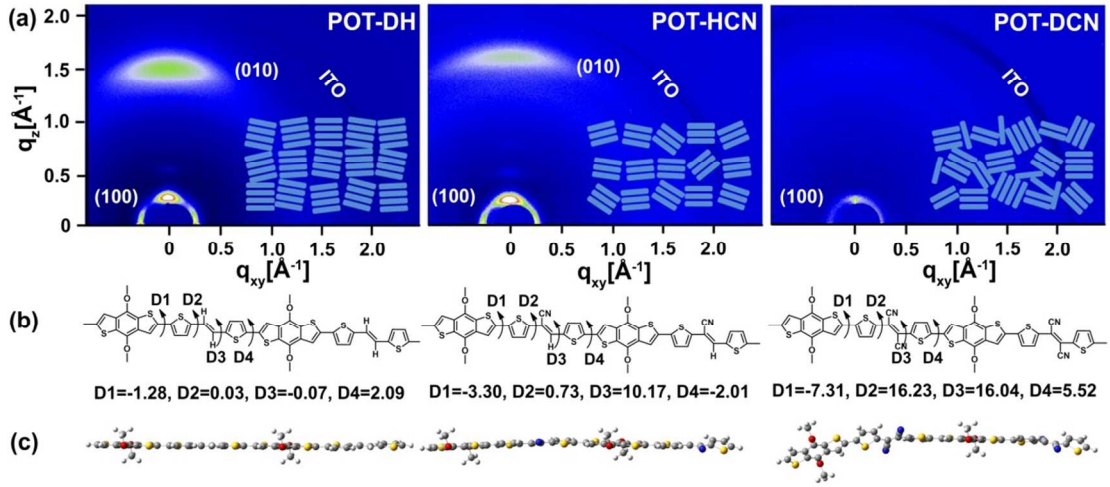

Fig. 3 (a) 2D grazing incidence X-ray diffration (GIXD) patterns of films of three polymers. Inset: schematic illustration of the orientation of the polymers. Calculated dihedral angles (b) of two repeating units of polymers and side view (c) of the model compounds, obtained at the DFT/B3LYP/6-31GD level.

on orientation is considered to be beneficial for charge transport in the device.[13] With increased CN–group number, the intensity of the (010) peak of polymers decreases with an order of **POT–DH** > **POT–HCN** > **POT–DCN**. It should be noted that no obvious signal of (010) peak can be observed for **POT–DCN**. The same results can also be obtained from 1D-graph of the GIXD (see Fig. S3 in the ESI†). Thus the inter–molecular packing of **POT–DCN** may be very poor, leading to a rather amorphous film (Fig. 3a, inset).

To confirm that, we further studied the structural properties of the polymers by theoretical computation at the B3LYP/6-31G*level on the model compound by using Gaussian 09 program suite. We calculated the dihedral angles between the two repeating units in **POT–DH**, **POT–HCN** and **POT–DCN** (Fig. 3b). The gradually increased dihedral angles (Fig. 3b) of the three polymers reveal that the planarity of the polymers is getting worse with the order of **POT–DH** > **POT–HCN** > **POT–DCN**. And the corresponding side–views of the molecules are shown in Fig. 3c, showing that the **POT–DCN** backbone is mostly twisted. These results of theoretical study are consistent with the results of GIXD measurement. It is clear that with increased number of CN–groups (from 0 to 2), the planarity of polymers becomes poorer, ascribed to the stronger steric hindrance of CN–group compared to that of hydrogen atom.[14]

Photovoltaic performance and hole mobilities

To elucidate the relationship between the CN–group number and the device performance, PSCs with the device structure of ITO/PEDOT:PSS/polymer:$PC_{61}BM$/LiF/Al were fabricated based on blends of **POT–DH**, **POT–HCN** or **POT–DCN** together with $PC_{61}BM$. Different solvents and different D–A weight ratios have been investigated to optimize the device performance (Table S1, see the ESI†). The photovoltaic parameters of PSCs at optimized conditions are summarized in Table 3 for comparison, with *I–V* curves shown in Fig. S4a (see the ESI†). Without using DIO, the V_{oc} of **POT−DH** based PSCs is 0.70 V, which is significantly lower than the 0.83 V of **POT−HCN** based device, likely due to the shallower HOMO levels. The *FF* of **POT−DH** and **POT−HCN** is 60.5% and 59.6% respectively, which is much higher than the 24% of **POT−DCN**. We attributed the difference to the worse inter−molecular packing of the latter, induced by the extra CN−group. After the addition of 2% DIO, PCEs of PSCs based on all polymers were improved significantly, mainly due to the hugely increased J_{sc}. Specifically, the **POT−HCN** based devices exhibit the highest PCE of 3.03% with V_{oc} = 0.79 V, J_{sc} = 7.05 mA/cm^2, and *FF* = 54.4%, which is over 10% higher than the 2.72% of **POT−DH** based ones (with V_{oc} = 0.70 V, J_{sc} = 6.77 mA/cm^2, and *FF* = 57.5%), mainly attributed to the larger V_{oc}. Note that with or without DIO, **POT−DCN** based devices show an extremely low PCE around 0.01%. Further optimization was performed by using $PC_{71}BM$ instead of conventional $PC_{61}BM$ to enhance the absorbance (Fig. 4a). As expected, the resultant solar cells exhibit increased J_{sc}, whereas other parameters including V_{oc} and *FF*, remain almost unchanged compared to devices using

Table 3 Summary of the optimized parameters of PSCs based on the polymer/$PC_{61}BM$ active layers (1:1.5, w/w) under the illumination of AM 1.5G, 100 mW cm^{-2}.

Polymer	Solvent	V_{oc} (V)	J_{sc} (mA/cm^2)	*FF* (%)	PCE (%)
POT-DH	CF	0.70	4.12	60.5	1.74
	CF+2% DIO	0.70	6.77	57.5	2.72
POT-HCN	CF	0.83	2.45	59.6	1.21
	CF+2% DIO	0.79	7.05	54.4	3.03
POT-DCN	CF	0.80	0.07	24.0	0.01
	CF+2% DIO	0.78	0.10	28.9	0.02

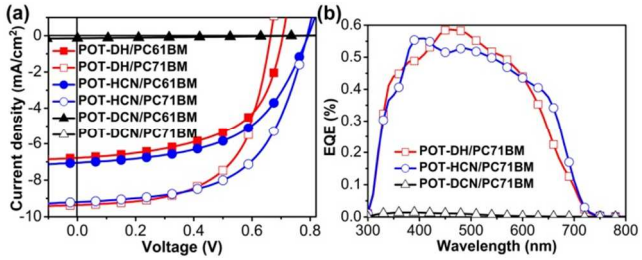

Fig. 4 (a) *I*–*V* curves of the PSCs based on polymer/$PC_{61}BM$ (1:1.5, w/w) with DIO and polymer/$PC_{71}BM$ (1:1.5, w/w) with DIO, under the illumination of AM1.5G, 100 mW cm^{-2}. (b) EQE spectra of the PSCs based on polymer/$PC_{71}BM$ blends.

Table 4 Photovoltaic parameters of the devices based on the active layers (1:1.5, w/w) containing 2% DIO as the processing additive.

Active layer	V_{oc} (V)	J_{sc} (mA/cm^2)	*FF* (%)	PCE (%)
POT-DH/$PC_{61}BM$	0.70	6.77	57.5	2.72
POT-DH/$PC_{71}BM$	0.66	9.36	60.3	3.73
POT-HCN/$PC_{61}BM$	0.79	7.05	54.4	3.03
POT-HCN/$PC_{71}BM$	0.79	9.20	57.9	4.21
POT-DCN/$PC_{61}BM$	0.78	0.10	28.9	0.02
POT-DCN/$PC_{71}BM$	0.77	0.14	28.8	0.03

$PC_{61}BM$ (Table 4). By using $PC_{71}BM$, the PCEs of the devices were improved dramatically from 2.72% to 3.73% for **POT−DH** and from 3.03% to 4.21% for **POT−HCN**, while almost no change for **POT−DCN** (from 0.02% to 0.03%). Fig. 4b shows the external quantum efficiency (EQE) curves of the PSCs based on polymer/$PC_{71}BM$ blends with 2% DIO. Maximum EQE values of 58.7% at 460 nm, 55.9% at 410 nm and 1.4% at 390 nm were recorded for the PSCs based on **POT−DH**, **POT−HCN** and **POT−DCN**, respectively. The J_{sc} calculated by integrating the EQE curve with an AM1.5G reference spectrum is within ~5% error compared to the corresponding J_{sc} obtained from the *J*-*V* curves.

The hole mobilities of the photosensitive layers were measured by the space charge limited current (SCLC) method using a device structure of ITO/PEDOT/polymer:$PC_{61}BM$/MoO_3(evaporated)/Al. The calculated hole mobilities based on polymer/$PC_{61}BM$ blends are 1.9×10^{-4}, 9.7×10^{-5} and 8.5×10^{-6} $cm^2V^{-1}s^{-1}$ for **POT−DH**, **POT−HCN** and **POT−DCN**, respectively. The results are consistent with the theoretical calculation, GIXD spectra and device performance.

Film morphology characterization

It is well-known that the performance of BHJ PSCs also depends on the physical interaction of the donor and acceptor components, which is directly manifested by the blend film morphology. An

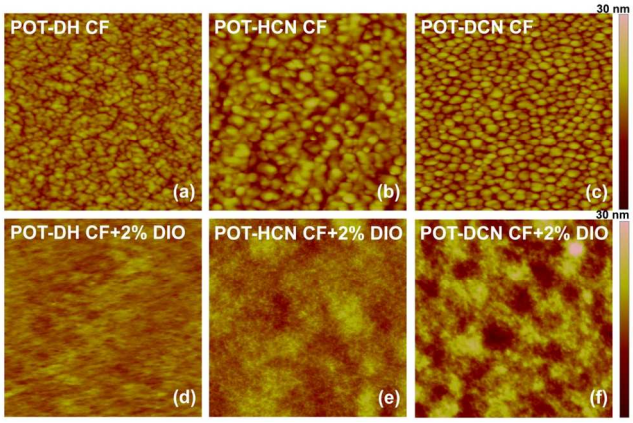

Fig. 5 AFM height images (5.0 μm × 5.0 μm) of polymer/$PC_{61}CM$ (1:1.5 w/w, CF) blend films without (a-c) or with DIO (d-f).

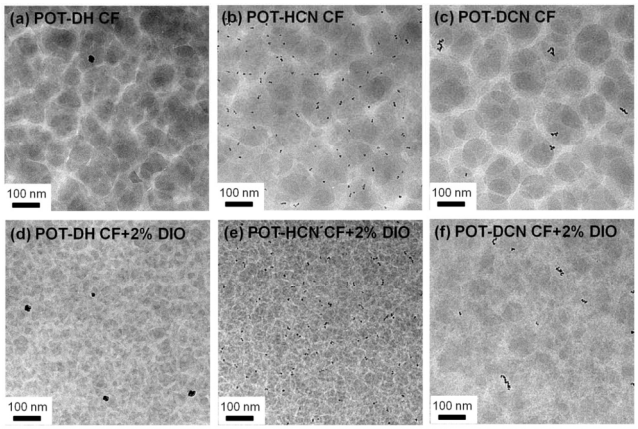

Fig. 6 TEM images of polymer/$PC_{61}BM$ blends (1:1.5 w/w) cast from chloroform (a-c) or chloroform with 2% DIO (d-f).

ideal BHJ PSC should possess a bicontinuous composite of donor and acceptor with a maximum interfacial area for exciton dissociation and a mean domain size commensurate with the exciton diffusion length (5–10 nm).[1b] The two components should phase-segregate on a suitable length scale to allow maximum ordering within each phase and thus effective charge transport in continuous pathways to the electrodes so as to minimize the recombination of free charges.[1b, 15] Such requirements necessitate that the favorable phase separation balance between the mixing and demixing of the two components can be achieved. Therefore, film morphology is a key parameter to explain the difference of photovoltaic performance. We further investigated the morphology of the polymer:$PC_{61}BM$ (1:1.5, w/w) blend films by employing a tapping–mode atomic force microscopy (AFM). As shown in Fig. 5, the average surface roughness (R_a) of the polymer/$PC_{61}BM$ blend films is determined to be 1.75, 2.35 and 2.39 nm for **POT−DH**, **POT−HCN** and **POT−DCN**, respectively. The domains on the surface of **POT−DCN**/$PC_{61}BM$ are evidently larger than that of the **POT−DH**/$PC_{61}BM$ film, indicating unfavorable phase separation. After the addition of DIO, R_a*s* of the corresponding blend films are determined to be 1.08, 1.60 and 2.93 nm respectively. Apparently, the addition of DIO makes the blend films of **POT−DH** and **POT−HCN** much smoother, but not for the film of **POT−DCN**. We confirmed the observation in transmission–electron microscopy (TEM) (Fig. 6) and high-angle annular dark–

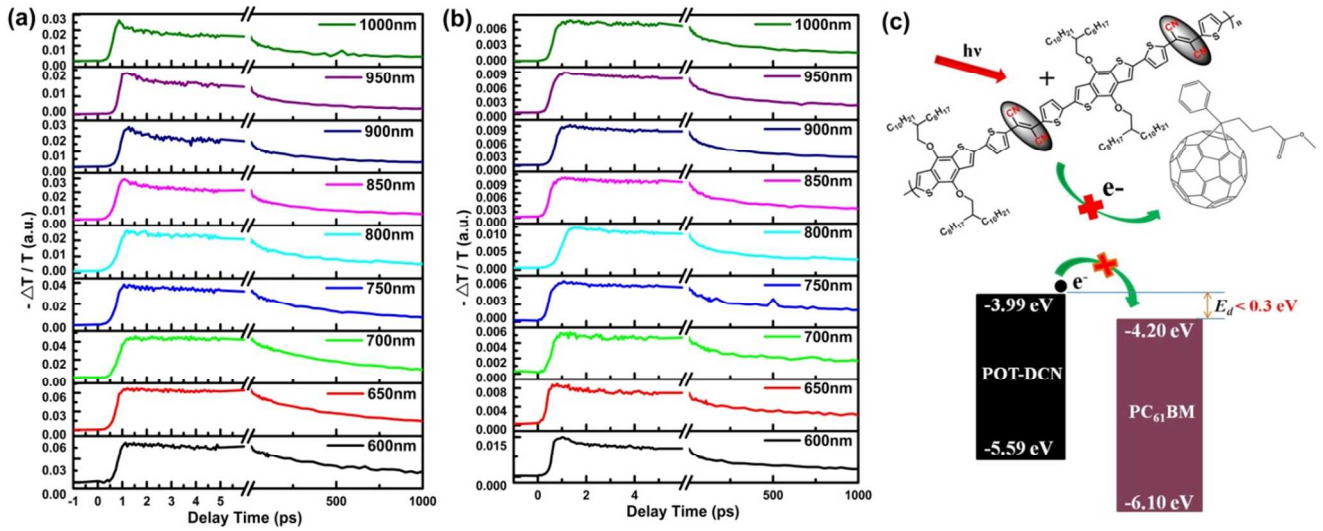

Fig. 7 Transient transmission spectra at different detection wavelengths: (a) for **POT-DCN** and (b) for **POT-DCN**/$PC_{61}BM$ blend, pulse width is 200 fs. Pumping wavelength is 400 nm. Pumping power is 60 μJ/cm^2; (c) Schematic diagram: the low LUMO energy level of **POT-DCN** prevented the electron transfer between polymer and $PC_{61}BM$.

field scanning transmission–electron microscopy (HAADF–STEM) (Fig. S5). As shown in Fig. 6, the polymer or fullerene–rich domains become much smaller after the addition of DIO, suggesting better mixing and more efficient charge transfer between the two components.[1b, 15] In STEM images, the contrast between polymer and fullerene is enhanced, leading to clearer observation of the morphology evolution. In Fig. S5, the sizes of polymer–rich domains in **POT−DCN**/$PC_{61}BM$ film is about 200 nm, which is too large for efficient exciton dissociation. In addition, the domains are separated from each other, indicating huge boundary resistance and very poor charge transport between domains. In contrary, the domains in the blend films of the other two polymers are interconnected and significantly smaller. After the addition of DIO, the domains in **POT−DCN** blend film are much smaller, but still not well connected, which accounts for the little performance improvement. For the other two polymers, the DIO leads to further reduced domains and formation of nanoscale networks between donor and acceptor materials, facilitating both exciton dissociation and charge transport in the blend film.[1b, 15] As a result, distinct improvements in photocurrent, from 4.12 and 2.45 to 6.77 and 7.05 mA/cm^2 were achieved for **POT−DH** and **POT−HCN** based devices, respectively. Therefore, the CN−group number has a large impact on the film morphology and thus affects the device performance.

Ultrafast transient transmission study

We further investigated the charge carrier dynamics in both pristine **POT−DCN** and **POT−DCN**/$PC_{61}BM$ blend films by ultrafast transient transmission study. As shown in Fig. 7a and 7b, the transient transmission spectra of **POT−DCN** and **POT−DCN**/$PC_{61}BM$ blends at different detection wavelengths (from 600 to 1000 nm, every other 50 nm) changed very slowly in the first 5 ps, which indicates that there is no obvious ultrafast charge transfer occurs between **POT−DCN** and $PC_{61}BM$. So the blend mixture showed almost no change in the transient relaxation process. This shows the inefficient charge transfer at the donor/acceptor interface,[16] which is well consistent with the extremely low photocurrent and device parameters. It can be concluded that the LUMO level of **POT−DCN** is too low to guarantee a sufficient downhill driving force to overcome the exciton binding energy for efficient electron transfer,[1c,17] as illustrated in Fig. 7c.

Conclusions

In conclusion, we investigated for the first time the effects of different CN−group numbers on the optoelectronic, structural, morphology and photovoltaic properties of three conjugated polymers **POT−DH**, **POT−HCN** and **POT−DCN**. With increased CN−group number, broader absorption, smaller optical bandgap and lower HOMO levels can be obtained. The planarity of polymers also decreases with increased CN−group, leading to different inter−molecular packing and morphology. The incorporation of two CN−groups results in poor morphology, inefficient charge transfer and very low device performance. The best PCE of 4.21% was demonstrated by **POT−HCN** with one CN−group. Thus we believe that, by controlling the number of introduced CN−groups, we can generally fine−tune the planarity and LUMO/HOMO levels of this class of polymers to achieve desired optoelectronic properties and morphology for high photovoltaic performance.

Acknowledgements

We acknowledge technical support from workers at Shanghai Synchrotron Radiation Facility (SSRF) on diffraction beamline (BL14B1). This work was supported by the National High Technology Research and Development Program of China (863 Program) (Grant No. 2011AA050520), the National Natural Science Foundation of China (Grant No. 61176054), the Priority Academic Program Development of Jiangsu Higher Education Institutions.

Notes and references

[a] *Institute of Functional Nano & Soft Materials (FUNSOM) & Collaborative Innovation Center of Suzhou Nano Science and Technology, Soochow University 199 Ren-Ai Road, Suzhou Industrial Park, Suzhou, Jiangsu 215123, P. R. China; Corresponding E-mail addresses: hqwang@suda.edu.cn (H.-Q. Wang); wlma@suda.edu.cn (W. L. Ma)*
[b] *Shanghai Ultra-precision Optical Engineering Center, and Key laboratory of Micro and Nano Photonic Structures (Ministry of Education), Department of Optical Science and Engineering, Fudan University, Shanghai 200433, China.*

† Electronic Supplementary Information (ESI) available: [details of any supplementary information available should be included here]. See DOI: 10.1039/b000000x/

1 (a) Y. F. Li, *Acc. Chem. Res.*, 2012, **45**, 723; (b) B. C. Thompson and J. M. J. Fréchet, *Angew. Chem., Int. Ed*., 2008, **47**, 58; (c) Y.-J. Chen, S.-H. Yang and C.-S. Hsu, *Chem. Rev.*, 2009, **109**, 5868; (d) J. W. Chen and Y. Cao, *Acc. Chem. Res.*, 2009, **42**, 1709; (e) G. Dennler, M. C. Scharber and C. J. Brabec, *Adv. Mater.*, 2009, **21**, 1323; (f) H. X. Zhou, L. Q. Yang and W. You, *Macromolecules*, 2012, **45**, 607.

2 (a) J. M. Szarko, J. C. Guo , Y. Y. Liang , B. D. Lee , B. S. Rolczynski , J. Strzalka , T. Xu , S. Loser , T. J. Marks , L. P. Yu , and L. X. Chen, *Adv. Mater.*, 2010, **22**, 5468; (b) E. G. Wang, L. T. Hou, Z. Q. Wang, Z. F. Ma, S. Hellström, W. L. Zhuang, F. L. Zhang, O. Inganäs and M. R. Andersson, *Macromolecules*, 2011, **44**, 2067; (c) A. T. Yiu, P. M. Beaujuge, O. P. Lee, C. H. Woo, M. F. Toney and J. M. J. Fréchet, *J. Am. Chem. Soc.*, 2012, **134**, 2180.

3 (a) J. Y. Yuan, Z. C. Zhai, H. L. Dong, J. Li, Z. Q. Jiang, Y. Y. Li and W. L. Ma, *Adv. Funct. Mater.*, 2013, **23**, 885. (b) J. Y. Yuan, X. D. Huang, F. J. Zhang, J. L. Lu, Z. C. Zhai, C.A. Di, Z. Q. Jiang and W. L. Ma, *J. Mater. Chem*., 2012, **22**, 22734; (c) Q. Peng, X. J. Liu D. Su, G. W. Fu, J. Xu and L. M. Dai, *Adv. Mater.*, 2011, **23**, 4554; (d) L. J. Huo, S. Q. Zhang, X. Guo, F. Xu, Y. F. Li and J. H. Hou, *Angew. Chem., Int. Ed.*, 2011, **50**, 9697; (e) L. J. Huo, J. H. Hou, S. Q. Zhang, H.-Y. Chen and Y. Yang, *Angew. Chem., Int. Ed.*, 2010, **49**, 1500; (f) J. Min, Z. G. Zhang, S. Y. Zhang and Y. F. Li, *Chem. Mater.*, 2012, **24**, 3247; (g) Q. Peng, Y. Y. Fu, X. J. Liu, J. Xu and Z. Y. Xie, *Poly. Chem.*, 2012, **3**, 2933; (h) Y. Zhang, L. Gao, C. He, Q. J. Sun and Y. F. Li, *Poly. Chem.*, 2013, **4**, 1474.

4 (a) H. X. Zhou, L. Q. Yang, S. C. Price, K. J. Knight and W. You, *Angew. Chem., Int. Ed.*, 2010, **49**, 7992; (b) N. Blouin, A. Michaud, D. Gendron, S. Wakim, E. Blair, R. N. Plesu, M. Belletête, G. Durocher, Y. Tao and M. Leclerc, *J. Am. Chem. Soc.*, 2008, **130**, 732; (c) J. Y. Yuan, X. D. Huang, H. L. Dong, J. L. Lu, T. Yang, Y. Y. Li, A. Gallagher and M. L. Ma, *Org. Electron.*, 2013, **14**, 635; (d) Y. Z. Lin, H. J. Fan, Y. F. Li and X. W. Zhan, *Adv. Mater.*, 2012, **24**, 3087; (e) H.-H. Cho, T.-E. Kang, K.-H. Kim, H. Kang, H.-J. Kim and B.-J. Kim, *Macromolecules*, 2012, **45**, 6415; (f) Y. Zhang, J. Y. Zou, H.-L. Yip, Y. Sun, J. A. Davies, K.-S. Chen, O. Acton and A. K.-Y. Jen, *J. Mater. Chem.*, 2011, **21**, 3895; (g) W. L. Zhuang, A. Lundin and M. R. Andersson, *J. Mater. Chem. A*, 2014, **2**, 2202; (h) J. H. Huang, Y. Zhao, W.W. He, H. Jia, Z. H. Lu, B. Jiang, C. L. Zhan, Q. B. Pei, Y. Q. Liu and J. N. Yao, *Polym. Chem.*, 2012, **3**, 2832.

5 (a) B. C. Thompson, Y.-G. Kim, T. D. McCarley and J. R. Reynolds, *J. Am. Chem. Soc.*, 2006, **128**, 12714; (b) H. Padhy, D. Sahu, D. Patra, M. K. Pola, J.-H. Huang, C.-W. Chu, K.-H. Wei and H.-C. Lin, *J. Polym. Sci., Part A: Polym. Chem.*, 2011, **49**, 3417; (c) J. H. Kwon, J.-Y. An, H. Jang, S. Choi, D. S. Chung, M.-J. Lee, H.-J. Cha, J.-H. Park, C.-E. Park and Y.-H. Kim, *J. Polym. Sci., Part A: Polym. Chem.*, 2011, **49**, 1119; (d) H.-G. Jeong, D. Khim, E. Jung, J.-M. Yun, J. Kim, J. Ku, Y. H. Jang and D.-Y. Kim, *J. Polym. Sci., Part A: Polym. Chem.*, 2013, **51**, 1029; (e) H.-Y. Chen, J.-L. Wu, C.-T. Chen and C.-T. Chen, *Chem. Commun.*, 2012, **48**, 1012; (f) F. Huang, K.-S. Chen, H.-L. Yip, S. K. Hau, O. Acton, Y. Zhang, J. D. Luo and A. K.-Y. Jen, *J. Am. Chem. Soc.*, 2009, **131**, 13886; (g) Z. F. Tan, I. Imae, K. Konaguchi, Y. Ooyama, J. Ohahita and Y. Harima, *Synth. Met.,* 2014, **187**, 30; (h) J. H. Huang, Y. Zhao, X. L. Ding, H. Jia, B. Jiang, Z. G. Zhang, C. L. Zhan, S. G. He, Q. B. Pei, Y. F. Li, Y. Q. Liu and J. N. Yao, *Polym. Chem.*, 2012, **3**, 2170.

6 (a) M. Neophytou, H. A. Ioannidou, T. A. Ioannou, C. L. Chochos, S. P. Economopoulos, P. A. Koutentis, G. Itskos and S. A. Choulis, *Poly. Chem.*, 2012, **3**, 2236; (b) S. C. Price, A. C. Stuart, L. Q. Yang, H. X. Zhou and W. You, *J. Am. Chem. Soc.*, 2011, **133**, 4625; (c) H. X. Zhou, L. Q. Yang, A. C. stuart, S. C. Price, S. B. Liu and W. You, *Angew. Chem., Int. Ed.*, 2011, **50**, 2995.

7 (a) J. H. Hou, H.-Y. Chen, S. Q. Zhang, R. I. Chen, Y. Yang, Y. Wu and G. Li, *J. Am. Chem. Soc.*, 2009, **131**, 15586; (b) Y. Y. Liang and L. P. Yu, *Acc. Chem. Res.*, 2010, **43**, 1227.

8 (a) R. Fitzner, C. Elschner, M. Weil, C. Uhrich, C. Körner, M. Riede, K. Leo, M. Pfeiffer, E. Reinold, E. M.-Osteritz and P. Bäuerle, *Adv. Mater.*, 2012, **24**, 675; (b) A. Gupta, A. Ali, A. Bilic, M. Gao, K. Hegedus, B. Singh, S. E. Watkins, G. J. Wilson, U. Bach and R. A. Evans, *Chem. Commun.*, 2012, **48**, 1889; (c) Y. Z. Lin, Z. G. Zhang, H. T. Bai, Y. F. Li and X. W. Zhan, *Chem. Commun.*, 2012, **48**, 9655; (d) S. H. Zeng, L. X. Yin, C. Y. Ji, X. Y. Jiang, K. C. Li, Y. Q. Li and Y. Wang, *Chem. Commun.*, 2012, **48**, 10627; (e) M. Charlotte, S. Gurunathan, A. Magali, K. Václav, S. Jiří, F. Pierre and R. Jean, *J. Org. Chem*., 2012, **77**, 2041.

9 J. L. Lu, J. Peng, Y. C. Wang, J. Y. Yuan, C. X. Sheng, H. Q. Wang and W. L. Ma, *Synth. Met.,* 2014, **188**, 57.

10 X. C. Wang, Y. P. Sun, S. Chen, X. Guo, M. J. Zhang, X. Y. Li, Y. F. Li and H. Q. Wang, *Macromolecules*, 2012, **45**, 1208.

11 M. Wang, X. W. Hu, P. Liu, W. Li, X. Gong, F. Huang and Y. Cao, *J. Am. Chem. Soc.*, 2011, **133**, 9638.

12 D. Sahu, H. Padhy, D. Patra, D. Kekuda, C.-W. Chu, I.-H. Chiang and H.-C. Lin, *Polymer*, 2010, **51**, 6182.

13 (a) C. Piliego, T. W. Holcombe, J. D. Douglas, C.-H. Woo, P. M. Beaujuge and J. M. J. Fréchet, *J. Am. Chem. Soc.*, 2010, **132**, 7595; (b) I. Osaka, M. Saito, T. Koganezawa and K. Takimiya, *Adv. Mater.*, 2013, **26**, 331; (c) X. Guo, S. R. Puniredd, M. Baumagarten, W. Pisula and K. Müllen, *Adv. Mater.*, 2013, 25, 5467.

14 L. J. Huo, Z. J. Li, X. Guo, Y. Wu, M. J. Zhang, L. Ye, S. Q. Zhang and J. H. Hou, *Poly. Chem.*, 2013, **4**, 3047.

15 (a) X. N. Yang and J. Loos, *Macromolecules*, 2007, **40**, 1353; (b) X. N. Yang, J. Loos, S. C. Veenstra, W. J. H. Vehees, M. M. Wienk, J. M. Kroon, M. A. J. Michels and R. A. J. Janssen, *Nano Lett.*, 2005, **5**, 579; (c) G. Li and Y. Yang, *Nat. Photon.*, 2012, **6**, 153. (d) J.-K. Lee, W. L. Ma, C. J. Brabec, J. Yuen, J.-S. Moon, J.-Y. Kim, K. Lee, G. C. Bazan and A. J. Heeger, *J. Am. Chem. Soc.*, 2008, **130**, 3619; (e) J. Peet, J. Y. Kim, N. E. Coates, W. L. Ma, D. Moses, A. J. Heeger and G. C. Bazan, *Nat. Mater.*, 2007, **6**, 497.

16 J. M. Szarko, B. S. Rolczynski, S. J. Lou, T. Xu, J. Strzalka, T. J. Marks, L. P. Yu and L. X. Chen, *Adv. Funct. Mater*., 2014, **24**, 10.

17 (a) L. J. A. Koster, V. D. Mihailetchi, and P. W. M. Blom, *Appl. Phys. Lett.,* 2006, **88**, 093511; (b) J. J. M. Halls, J. Cornil, D. A. dos Santos, R. Silbey, D.-H. Hwang, A. B. Holmes, J. L. Brédas and R. H. Friend, *Phys. Rev. B* 1999, **60**, 5721.

Graphical Abstract